RAA 2018 Vol. **18** No. **7**, 87(12pp) doi: 10.1088/1674–4527/18/7/87

http://www.raa-journal.org *http://iopscience.iop.org/raa*

Research in Astronomy and Astrophysics

Spectroscopic and photometric studies of a candidate pulsating star in an eclipsing binary: V948 Her

Filiz Kahraman Aliçavuş

Faculty of Sciences and Arts, Physics Department, Çanakkale Onsekiz Mart University, 17100, Çanakkale, Turkey; *filizkahraman01@gmail.com, filizkahraman@comu.edu.tr*

Received 2018 March 1; accepted 2018 April 18

Abstract Eclipsing binary stars with a pulsating component are powerful tools that allow us to probe the stellar interior structure and the evolutionary statuses with a good accuracy. Therefore, in this study, spectroscopic and photometric examinations of an eclipsing binary system V948 Her are presented. The primary component of the system is classified to be a candidate δ Scuti variable in the literature. The fundamental stellar, atmospheric and orbital parameters, and the surface abundance of the star were determined and the pulsation behaviour was investigated in this study. The orbital parameters were derived by the analysis of radial velocity and SuperWASP light curves. The spectral classification was found to be F2V. The initial atmospheric parameters of the primary component were derived by analysis of the spectral energy distribution and hydrogen lines. The final atmospheric parameters and chemical abundances of the primary component were obtained by using the method of spectrum synthesis. As a result, the final atmospheric parameters were determined as $T_{\rm eff}= 7100{\pm}200\,$K, $\log g= 4.3{\pm}0.1$ cgs and $\xi = 2.2 \pm 0.2\,$km s^{-1}. The surface abundance was found to be similar to solar. The fundamental stellar parameters of both components were also obtained to be $M = 1.722 \pm 0.123$, $0.762 \pm 0.020\,M_{\odot}$, $R = 1.655 \pm 0.034$, $0.689 \pm 0.016\,R_{\odot}$ for primary and secondary components, respectively. The pulsation characteristic of the primary component was examined using SuperWASP data and the pulsation period was found to be $\sim$0.038 d. The position of the primary pulsating component was also obtained inside the instability strip of δ Sct stars. The primary component of V948 Her was defined to be a δ Sct variable.

Key words: techniques: photometric, spectroscopic — stars: binaries: eclipsing — stars: variables: δ Scuti — stars: individual (V948 Her)

1 INTRODUCTION

A significant amount of stars is in binary or multiple systems (Alfonso-Garzón et al. 2014; Duchêne & Kraus 2013). Binary systems, in particular eclipsing binaries, are very valuable objects because they give us an opportunity to determine the fundamental stellar parameters (e.g. mass, radius) with good accuracy. Eclipsing binary stars include components that have a wide range of spectral types (e.g. Shokry et al. 2018; Kjurkchieva & Vasileva 2018; Koo et al. 2017). Therefore, some of these components can be found inside an instability strip of a pulsating star group such as δ Scuti (δ Sct), γ Doradus or β Cephei variables. The existence of pulsating stars in eclipsing binaries has been known for about 50 years. Until now, lots of pulsating stars in eclipsing binaries have been found, especially with the contribution of space missions (e.g. Liakos 2017; da Silva et al. 2014).

One of the most common pulsating variables in eclipsing binaries is δ Sct stars. δ Sct variables are placed in the lower part of the classical instability strip, and they have a spectral type in a range of A0–F5 (Chang et al. 2013). These variables pulsate in radial and non-radial pressure and gravity modes, mostly in a frequency range of $5 - 50$ d^{-1} (Breger 2000). The first list of δ Sct stars in binaries was given by Rodríguez et al. (2000). In this list, there were only 15 stars. In the following years, Soydugan et al. (2006a) published a new list of eclipsing binaries with a δ Sct component. In this study, a relationship between the pulsation and orbital period was announced. According to this relation, the pulsation periods of δ Sct components increase with a growing orbital period. The pulsation – orbital period relation has been improved by new discoveries (Kahraman Aliçavuş et al. 2017b; Liakos et al. 2012). Furthermore, this relation was theoretically revealed by Zhang et al. (2013). They showed that the pulsation period changes according to the orbital period, the mass ratio of components and also the filling factor of the pulsating component in an eclipsing binary. Additionally, an inverse relationship between the pulsation period and surface gravity was obtained for δ Sct components in eclipsing binaries (Kahraman Aliçavuş et al. 2017b; Liakos & Niarchos 2017; Liakos et al. 2012). In a recent study, differences between single and eclipsing binary member δ Sct stars were examined in detail (Kahraman Aliçavuş et al. 2017b). In this study, it was shown that single δ Sct stars pulsate with longer pulsation period and higher amplitude compared to δ Sct components in eclipsing binaries. It was also found that single δ Sct stars rotate faster.

Asteroseismology is the most important way to infer stellar interior structure in detail. The combination of asteroseismic examinations with eclipsing binary analysis offers us excellent power to understand the stellar interior structure and evolution. Therefore, eclipsing binaries with δ Sct components are crucial tools. Hence, in this study, analysis of one candidate of this type of object is presented. Detailed spectroscopic and photometric studies of V948 Her are given.

V948 Her is an eclipsing binary system and its variability was first revealed by *Hipparcos* (ESA 1997). The orbital period of the system is 1.275204 d (Kreiner 2004) and the system was defined to be a detached eclipsing binary (Liakos & Niarchos 2012). The primary component of V948 Her was listed to be a candidate δ Sct star in an eclipsing binary (Soydugan et al. 2006b). Light curve analysis of the system was previously presented by Liakos & Niarchos (2012a). In this study, they also examined the star's pulsation characteristic. However, they found no significant result.

In the present study, information about the used photometric and spectroscopic data is given in Section 2. Spectroscopic analysis of V948 Her is presented in Section 3. Determination of the radial velocities of the system and analysis of the radial velocity curve are presented in Section 3.1. The spectral classification, spectral energy distribution (SED), hydrogen line analysis and determination of the final atmospheric parameters are introduced in Section 3.2. In Section 3.3, the chemical abundance analysis is given. An updated light curve analysis for V948 Her is provided in Section 4. Examination of the pulsation characteristics of the primary component of V948 Her is discussed in Section 5. A discussion and conclusion are also given in Section 6.

2 PHOTOMETRIC AND SPECTROSCOPIC DATA

Photometric data of V948 Her were taken from the Super Wide Angle Search for Planets (SuperWASP) archive[1]. SuperWASP is a ground-based programme for detecting exoplanets by the transit method (Pollacco et al. 2006). It also provides photometric data on a wide range of variable stars. The programme consists of a two-site campaign. One is located on the island of La Palma and the other is located in South Africa. The cameras of SuperWASP observe the sky in both hemispheres except for the Galactic disk. Each SuperWASP camera takes data from broadband filters that have a wavelength range of 4000−7000 Å. The precision of SuperWASP data can reach 0.004 mag for stars brighter than 9.4 mag (Pollacco et al. 2006). The SuperWASP data on V948 Her ($V = 8.91$ mag) comprise approximately 13 000 data points taken from 2004 to 2008. These data were used in analysis of the light curve and to examine the pulsation behaviour of the system.

The spectroscopic data were taken from the ELODIE archive[2] (Moultaka et al. 2004). ELODIE is an échelle spectrograph which was mounted at the 1.93-m telescope of the Observatoire de Haute Provence (France). The spectrograph was used for about 12 years between 1993 and 2006. It provided many spectra with a resolving power of ∼42 000. The wavelength range of spectra covers approximately from 4000 to 6800 Å. The reduction of spectra was executed automatically by a dedicated pipeline. V948 Her has 13 spectra in the ELODIE archive. These spectra were taken between 1999 and 2002, and they have signal-to-noise (S/N) ratios from ∼20 to 90. In the following analysis, one of the spectra was not taken into account due to its low S/N. Twelve

[1] *http://www.superwasp.org/*
[2] *http://atlas.obs-hp.fr/elodie/*

spectra were used in this study to determine the star's radial velocity curve, atmospheric parameters and chemical abundance.

3 SPECTROSCOPIC ANALYSIS

Using the star's ELODIE spectra, first the radial velocity ($v_{\rm r}$) curve of the system was obtained. Then spectral classification was performed. The SED of the primary star was obtained to derive the initial atmospheric parameter for further spectroscopic analysis. The atmospheric parameters of the primary component of V948 Her were determined from the analysis of hydrogen and metal lines. Finally, the chemical composition of the primary component was derived. In all spectroscopic analyses, ATLAS9 model atmospheres (Kurucz 1993) were used and the synthetic spectra were generated using the SYNTHE code (Kurucz & Avrett 1981).

3.1 Radial Velocity Analysis

The orbital parameters (eccentricity e, argument of periapsis ω, velocity of the center of mass of the system V_γ, mass ratio q[3], mass function f[4], $a$sin$i$ [a and i are semi-major axis and inclination, respectively], and the amplitude of $v_{\rm r}$ for the star with respect to the center of mass of the binary K) are obtained by the analysis of radial velocity curves of systems. To obtain these orbital parameters for V948 Her, the $v_{\rm r}$ values of the system were calculated using the FXCOR task in the NOAO/IRAF[5] package. This task derives the $v_{\rm r}$ values of components taking into account the cross-correlation method. In the radial velocity analysis, the ELODIE spectrum of a well-known radial velocity standard star HD 50692 ($v_{\rm r} = -15.5$ km s^{-1}, Udry et al. 1999) was adopted as a template. During the analysis, the wavelength range of $4400 - 5000$ Å was used. As a result of the analysis, only the $v_{\rm r}$ values for the primary component were derived, and the spectral lines coming from the secondary component cannot be seen in any spectra. For a given spectrum, a $v_{\rm r}$ value with a big uncertainty was calculated. This value was also not compatible with the other $v_{\rm r}$ measurements, therefore it was not used in the analysis. The results of 11 measured $v_{\rm r}$ values of the primary component are listed in Table A.1.

[3] $M_{\rm secondary}/M_{\rm primary}$ where M denotes the mass
[4] $f = (M_{\rm secondary} \sin i)^3 / (M_{\rm primary} + M_{\rm secondary})^2$
[5] *http://iraf.noao.edu/*

Table 1 The Results of Radial Velocity Analysis for V948 Her

Parameter	Value
P (d)^a	1.2752040
T_0^a (HJD)	2452001.56024
e	0.00000 ± 0.00467
ω (deg)	123.741 ± 0.333
γ (km s^{-1})	–6.157 ± 0.327
K_1 (km s^{-1})	81.493 ± 0.422
$a_1 \sin i$ (10^6 km)	1.4290 ± 0.0074
$f(m_1, m_2)$ ($M_\odot$)	0.0715 ± 0.0016
χ^2	37.431
Time span (d)	1085.1080
rms$_1$ (km s^{-1})	2.451

Notes: The subscripts "1" and "2" represent the primary and secondary component, respectively. ^{a} Fixed parameter.

To analyse the $v_{\rm r}$ curve of the system, `rvfit` code[6] (Iglesias-Marzoa et al. 2015) was used. The `rvfit` analyses $v_{\rm r}$ curves of single and double-lined binaries or exoplanets using the adaptive simulated annealing algorithm (Ingber 1996). This algorithm fits the orbital parameters, the orbital period P and the time of periastron passage T_0. Those parameters for V948 Her were derived by running the `rvfit`. In this analysis, the P and T_0 parameters were assumed to be 1.275204 d and 2452001.56024 (Heliocentric Julian Date, HJD) (Kreiner 2004), respectively and they were fixed during the analysis. The obtained results are given in Table 1 and a comparison of the calculated $v_{\rm r}$ curve with the derived $v_{\rm r}$ values is shown in Figure 1.

3.2 Atmospheric Parameters

To derive the atmospheric parameters (effective temperature $T_{\rm eff}$, surface gravity $\log g$ and microturbulent velocity ξ) of the primary star, a few different methods were used and the average spectrum of the system was taken into account. First, initial information about the atmospheric parameters was obtained with the spectral classification. Second, the SED and hydrogen lines analyses were carried out to determine the initial $T_{\rm eff}$ value of the star. The final atmospheric parameters were derived by the analysis of metal lines using the spectrum synthesis method. According to the $v_{\rm r}$ analysis, the light contribution of the secondary component in the spectra is negligible, hence all analyses were carried out only for the primary component of V948 Her.

[6] *http://www.cefca.es/people/riglesias/rvfit.html*

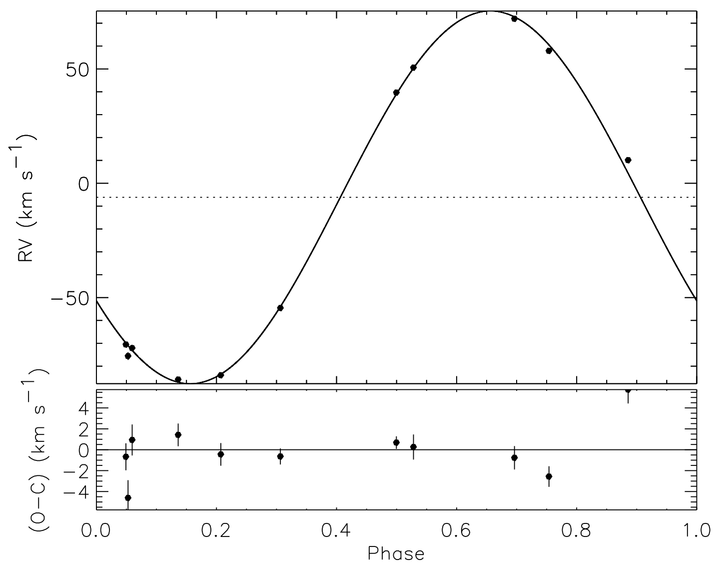

Fig. 1 *Upper panel*: comparison of the calculated $v_{\rm r}$ curve (*solid line*) with the derived $v_{\rm r}$ values (*dots*). *Lower panel*: residuals.

(i) *Spectral Classification*: The spectral classification was first carried out to obtain preliminary information about the star's $T_{\rm eff}$, $\log g$ and surface chemical peculiarities. In spectral classification, the spectral and luminosity types are determined by comparing the spectra of some standard stars used for spectral classification with the spectra of observed stars. In this analysis, the spectral and luminosity types of the primary component of V948 Her were determined by considering the minimum difference between the spectra of standard stars (Gray et al. 2003) and V948 Her. During the classification, the Hβ, Hγ and metal lines in the wavelength range of $\sim$4000−4500 Å were taken into account. As a result, the spectral classification of V948 Her was found to be F2V and no chemical peculiarities were determined.

(ii) *Spectral Energy Distribution*: SED analysis was carried out to derive an initial $T_{\rm eff}$ value for the primary component. As SED is strongly affected by the interstellar reddening $E(B-V)$, this value was calculated from the interstellar extinction map (Amôres & Lépine 2005). The *Gaia* parallax[7] (Gaia Collaboration et al. 2016) and the Galactic coordinates of V948 Her were used to obtain the $E(B-V)$ value. As a result, $E(B-V)$ was found to be 0.0106 ± 0.0021 mag. To produce the SED for the primary component of V948 Her, the SED code written by Dr. D. Shulyak (private communication) was used. The code utilizes the ATLAS9 model atmospheres (Kurucz 1993) to generate the SEDs and fits the calculated SEDs to spectrophotometric and photometric values of systems. It gives results taking into account the minimum differences between the calculated and given fluxes. For the SED analysis of V948 Her, only BV (Mermilliod et al. 1997) and 2MASS (Cutri et al. 2003) colours could be used. The $\log g$ and metallicity values were obtained as 4.0 cgs and 0.0 dex, respectively. Subsequently, the SED $T_{\rm eff}$ value was found to be 6710 ± 120 K. The SED fit is shown in Figure 2.

(iii) *Hydrogen Line Analysis*: The SED $T_{\rm eff}$ value was improved by performing hydrogen lines analysis. During the analysis, $\log g$ and metallicity were assumed to be 4.0 cgs and 0.0 dex, respectively. In the analysis, the $T_{\rm eff}$ value was searched in a range of $6500 - 7500$ K with 100 K steps. The Hβ, Hγ and Hδ lines were analysed simultaneously. Considering the minimum difference between the calculated and observed spectra, the hydrogen $T_{\rm eff}$ value was found to be 7000 ± 200 K. A comparison between the theoretical and observed spectra is illustrated in Figure 3.

(iv) *Final Atmospheric Parameters*: Final atmospheric parameters of the primary component of V948 Her were obtained by utilizing the excitation and ionization potential balance of metal lines. As the iron (Fe) lines are more available in this $T_{\rm eff}$ ($\sim$7000 K), Fe

[7] 6.15 ± 0.26 mas

lines were used in the analysis. The combined spectrum of the star was divided into parts line by line for the analysis. In case of blended lines, the parts were obtained considering the normalisation level. The analysis was carried out by using the spectrum synthesis method for ranges $6500-7800$ K, $3.5-4.5$ cgs and $1.5-3.0$ km s^{-1}of $T_{\rm eff}$, $\log g$ and ξ, respectively. The $T_{\rm eff}$, $\log g$ and ξ values were searched with steps of 100 K, 0.1 cgs and 0.1 km s^{-1}respectively. During the analysis, 117 spectral parts were analysed separately for the given ranges of the atmospheric parameters.

After the metal lines analysis was performed, the $T_{\rm eff}$ and $\log g$ values of the star were derived by taking into account the correlations between excitation-ionization potential and Fe abundances. The ξ parameter was also determined considering the relation between the depths and abundances of Fe lines. The mentioned correlations should equal zero when atmospheric parameters are accurate (for details see Kahraman Aliçavuş et al. 2016). The obtained final atmospheric parameters of V948 Her are given in Table 2.

Table 2 The Final Atmospheric Parameters and $v\sin i$ for the Primary Component of V948 Her

$T_{\rm eff}$ (K)	$\log g$ (cgs)	ξ (km s^{-1})	$v\sin i$ (km s^{-1})
7100 ± 200	4.3 ± 0.1	2.2 ± 0.2	68 ± 6

3.3 Chemical Abundance Determination

The chemical abundance of the primary component of V948 Her was derived taking into account the final atmospheric parameters. In this analysis, the spectrum synthesis method was used and all spectral parts were analysed. The line identification of the spectral parts was made using the line list of Kurucz[8]. Abundances of the identified chemical elements in each spectral part were adjusted until a theoretical spectrum fit the observed one. During the analysis, the $v\sin i$ value was also determined. Although elemental abundances and $v\sin i$ value were obtained from each spectral part, their average values are given in Table 3 and Table 2, respectively. Comparison of the theoretical and observed spectra for three spectral parts are shown in Figure 4. Chemical abundance distribution of the star is also demonstrated in Figure 5.

Uncertainties of the chemical elemental abundances were obtained considering all sources of uncertainty.

[8] *kurucz.harvard.edu/linelists.html*

Table 3 Abundances of individual elements of the primary star and Sun (Asplund et al. 2009). Number of the analysed spectral parts is given in parentheses.

Elements	Star abundance	Solar abundance
$_{6}$C	8.69 ± 0.52 (3)	8.43 ± 0.05
$_{11}$Na	6.36 ± 0.53 (1)	6.24 ± 0.04
$_{12}$Mg	7.59 ± 0.53 (4)	7.60 ± 0.04
$_{14}$Si	7.36 ± 0.52 (9)	7.51 ± 0.03
$_{20}$Ca	6.23 ± 0.50 (10)	6.34 ± 0.04
$_{21}$Sc	2.94 ± 0.52 (5)	3.15 ± 0.04
$_{22}$Ti	4.91 ± 0.53 (29)	4.95 ± 0.05
$_{23}$V	4.54 ± 0.53 (2)	3.93 ± 0.08
$_{24}$Cr	5.58 ± 0.55 (25)	5.64 ± 0.04
$_{25}$Mn	4.97 ± 0.54 (9)	5.43 ± 0.05
$_{26}$Fe	7.28 ± 0.52 (91)	7.50 ± 0.04
$_{28}$Ni	6.12 ± 0.57 (18)	6.22 ± 0.04
$_{29}$Cu	3.57 ± 0.53 (1)	4.19 ± 0.04
$_{30}$Zn	4.31 ± 0.53 (1)	4.56 ± 0.05
$_{38}$Sr	3.05 ± 0.53 (1)	2.87 ± 0.07
$_{40}$Zr	2.46 ± 0.53 (1)	2.58 ± 0.04

Adopted atmospheric models, S/N and the resolving powers of instruments are some of these sources. Uncertainties caused by these factors were taken from Kahraman Aliçavuş et al. (2017a). Errors in atmospheric parameters also introduce uncertainties in chemical abundances. Therefore, those uncertainties were calculated and it turned out that $T_{\rm eff}$ error introduces about 0.12 dex uncertainties in chemical abundance. The errors of $\log g$ and ξ cause 0.02 and 0.04 dex uncertainties, respectively. All sources of uncertainty were taken into account and the results are given in Table 3.

4 LIGHT CURVE ANALYSIS

The light curve of the eclipsing binary star V948 Her was taken from the SuperWASP project. Scattering points in the light curve were cleaned and it was normalised to 1 for the analysis. Light curve analysis of V948 Her was previously performed by Liakos & Niarchos (2012a). In this analysis, they defined the star to be a detached binary system. While they adopted the primary component's $T_{\rm eff}$ value to be 7000 K, which is very similar to the $T_{\rm eff}$ obtained in this study, they found the system's q value to be 0.27 ± 0.03.

The present light curve analysis was performed using the Wilson$-$Devinney code (Wilson & Devinney 1971). The light and radial velocity curves of the system were analysed simultaneously. The primary star's $T_{\rm eff}$ was taken to be 7100 K from the spectral analysis of this study, and it was fixed during the analysis. Additionally,

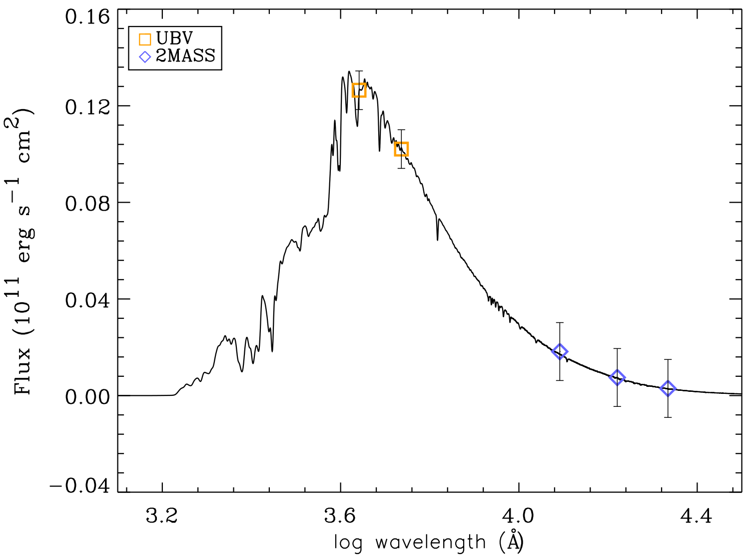

Fig. 2 The SED fit for the primary component of V948 Her.

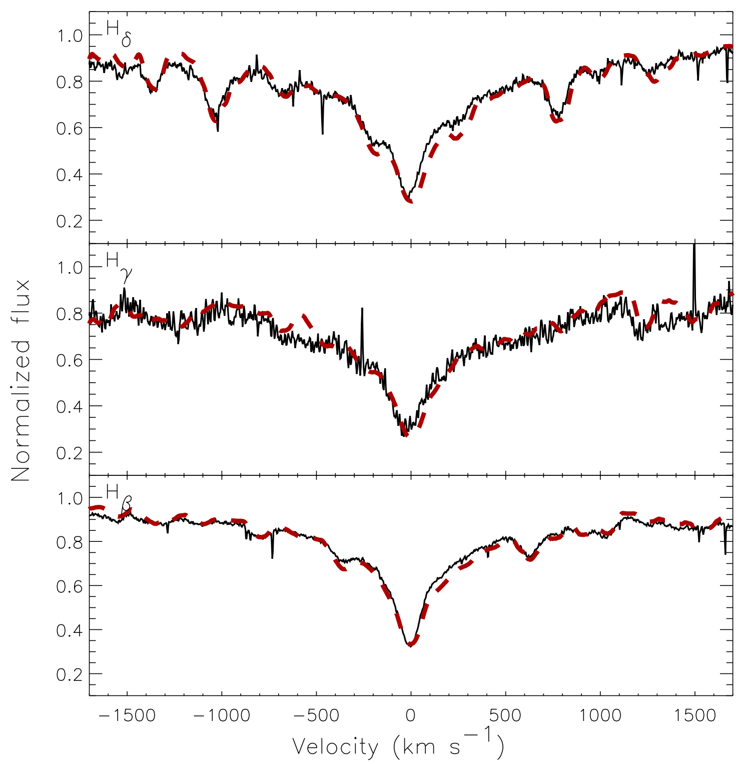

Fig. 3 Comparison of the observed (*solid lines*) hydrogen lines with the calculated spectra (*dashed lines*) for 7000 K.

the bolometric albedos (Ruciński 1969) and the bolometric gravity-darkening coefficients (von Zeipel 1924) were set to be 0.5 and 0.32 for convective atmospheres, respectively. The logarithmic limb darkening coefficients were taken from van Hamme (1993) and were fixed in the analysis. Considering the results of the radial velocity analysis, a circular orbit ($e = 0$) was assumed. Furthermore, synchronous rotation was accepted. The $T_{\rm eff}$ of the secondary component, the surface potentials ($\Omega_{\rm primary,secondary}$), the phase shift ($\phi$), q, i, a and V_γ were calculated and the analysis was carried out taking into account the detached binary approach.

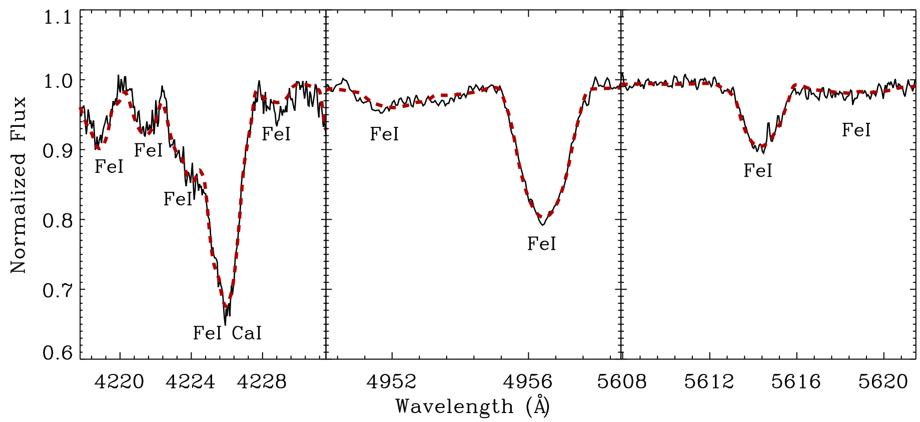

Fig. 4 Comparison of the theoretical (*dashed line*) and observed (*solid line*) spectra.

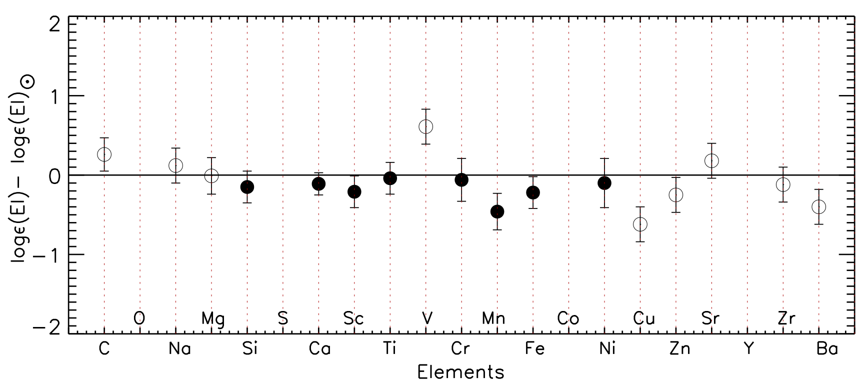

Fig. 5 The differences between the derived chemical abundances of the star and solar values (Asplund et al. 2009) as a function of elements. *Filled circles* show the difference in the elemental abundances that were obtained from at least five or more lines, while others represent cases with less than five lines.

In this analysis, first the q value was searched considering the sum of squared residuals ($\Sigma(O-C)^2$). The q value was fixed with a step of 0.1 from 0.1 to 1, and analysis was performed for each q value. The result of this research is shown in Figure 6. As can be seen from the figure, $\Sigma(O-C)^2$ is a minimum for $q \approx 0.4$. Therefore, the q value of the system was searched for around this minimum value.

During the analysis, no third light contribution was found. The results of the light curve analysis are listed in Table 4, and the fit of the theoretical and SuperWASP light curves is illustrated in Figure 7. Roche geometry of V948 Her is also shown in Figure 8.

Table 4 Results of Light Curve Analysis for V948 Her

Parameter	Value
a ($R_\odot$)	6.7160 ± 0.0535
i (°)	86.896 ± 0.044
V_γ (km s^{-1})	-6.210 ± 0.002
$T^a_{\rm primary}$ (K)	7100 ± 200
$T_{\rm secondary}$ (K)	4430 ± 250
$\Omega_{\rm primary}$	4.5205 ± 0.0048
$\Omega_{\rm secondary}$	5.5838 ± 0.0101
Phase shift	0.00040 ± 0.00004
q	0.443 ± 0.013
$g_{\rm primary,secondary}$	0.32, 0.32
$A_{\rm primary,secondary}$	0.5, 0.5
$L_{\rm primary}$ / ($L_{\rm primary} + L_{\rm secondary}$)	0.9811 ± 0.0043
$L_{\rm secondary}$ / ($L_{\rm primary} + L_{\rm secondary}$)	0.0189 ± 0.0050

5 PULSATION BEHAVIOR

V948 Her was defined to be a candidate δ Sct star in an eclipsing binary (Soydugan et al. 2006b). Ground-based photometric observations of the system were carried out by Liakos & Niarchos (2012a). However, they did not find convincing pulsation behaviour. According

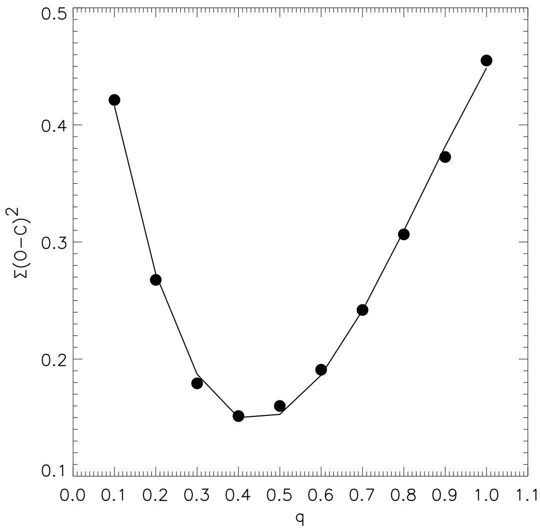

Fig. 6 Sum of squared residuals as a function of q.

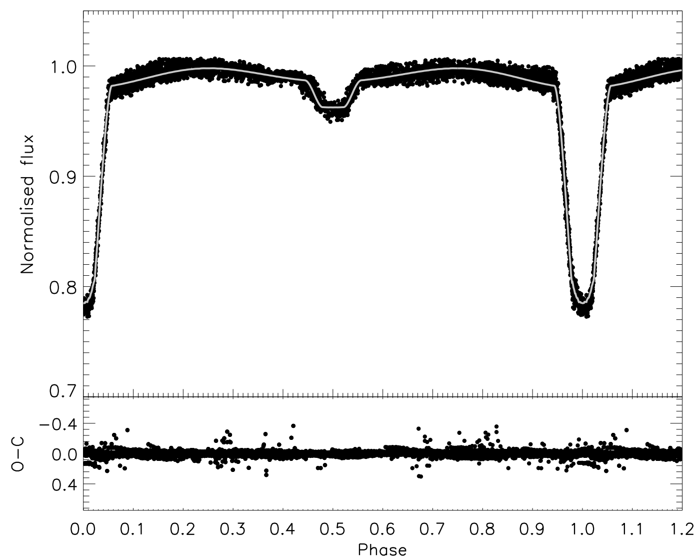

Fig. 7 Upper panel: comparison of the theoretical (*gray*) and the observed (*black*) light curves. Lower panel: residuals.

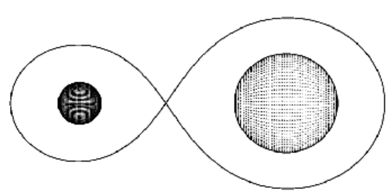

Fig. 8 Roche geometry of V948 Her at orbital phase 0.75.

to the correlation between the pulsation and orbital period (Kahraman Aliçavuş et al. 2017b), the primary component of V948 Her should pulsate with a period of ∼0.036 d. When the SuperWASP light curve was examined, in only a few days, the pulsation behaviour of the primary component of V948 Her was clearly seen, as shown in Figure 9. In the figure, the pulsations can be clearly seen in the maximums of the light curve and even during the eclipse. According to this behaviour, the pulsation period of the primary component of V948 Her was estimated to be ∼0.038 d which is very similar to the obtained period from the pulsation−orbital period correlation. However, to acquire an accurate result for this system, high-quality photometric observations are needed.

6 DISCUSSION AND CONCLUSIONS

In this study, detailed spectroscopic and photometric studies of V948 Her were presented. The orbital parameters of the system were obtained by analysis of the radial velocity and light curves. According to the result of light curve analysis, it was shown that the light contribution of the primary component in total is about 98% and the spectral lines of the secondary component cannot be seen in any spectra. Therefore, only the radial velocities of the primary component were measured in the study. The obtained radial velocities were analysed and the results were improved by simultaneous analysis of radial and light curves. Using the results of this analysis, the astrophysical parameters of V948 Her were derived as listed in Table 5. By utilizing these astrophysical parameters, as well as the interstellar absorption value $A_{\rm v}$ (Schlafly & Finkbeiner 2011) and the bolometric correction (Cox et al. 2000) for V948 Her, the distance of the system was calculated to be $155{\pm}10$ pc, which is compatible with the distance provided by *Gaia* (∼162 pc, Gaia Collaboration et al. 2016) within errors.

The atmospheric parameters and the chemical abundances of the primary component were obtained. According to the results of these analyses, $T_{\rm eff}$ and $\log g$ values are 7100 K and 4.3 cgs, respectively and the star has nearly solar abundance. Using the fundamental parameters, the $\log g$ value of the primary component was also calculated to be 4.24 ± 0.04 cgs, which is very similar to the spectroscopic $\log g$.

The pulsation behaviour of the primary component of V948 Her was also investigated. The pulsation period was found to be ∼0.038 d. However, the star needs high-quality observations to determine a more exact pulsation period. The position of the pulsation component in the pulsation−orbital period correlation is demonstrated in Figure 10. As can be seen from the figure, the star is compatible with the relation. In the study of Kahraman Aliçavuş et al. (2017b), more relations between the pulsation period and other parameters (e.g. $T_{\rm eff}$, $\log g$, M and R) of the δ Sct stars in eclipsing binaries were given. Using these relations, $T_{\rm eff}$, $\log g$, M and R parameters of the primary component of V948 Her were calculated. As a result of these calculations, the parameters were found to be $T_{\rm eff} = 7990 \pm 300$ K, $\log g = 4.11 \pm 0.20$ cgs, $M = 2.0 \pm 0.2\,M_\odot$ and $R = 2.24 \pm 0.2\,R_\odot$. Only the $\log g$ parameter is compatible with the spectroscopic $\log g$ within error. The other parameters differ from the obtained values in this study. There are a few reasons for these results. First, the pulsation period of V948 Her is not exact. Second, $T_{\rm eff}$ values used to check the $T_{\rm eff}$ − pulsation period correlation are mostly photometric values and not so accurate. Therefore, the error in the $T_{\rm eff}$ derived from the $T_{\rm eff}$ − pulsation period relation is big. Additionally, M and R are also generally assumed to be based on photometric results and in the correlations of the pulsation period − M and R, those photometric parameters were used to check the relationships (Kahraman Aliçavuş et al. 2017b). Hence, some correlations given in Kahraman Aliçavuş et al. (2017b) should be examined again by only using the spectroscopic results.

Table 5 Astrophysical Parameters for V948 Her

Parameter	Primary	Secondary
M ($M_\odot$)	1.722 ± 0.123	0.762 ± 0.020
R ($R_\odot$)	1.655 ± 0.034	0.689 ± 0.016
L ($L_\odot$)	6.233 ± 0.749	0.164 ± 0.031
$M_{\rm bolometric}$ (mag)	2.763 ± 0.691	6.715 ± 1.327

The position of the primary pulsating star is shown in the Hertzsprung-Russell (H-R) diagram in Figure 11. The star is placed inside the δ Sct instability strip and it is close to the red edge. In this part of the H-R diagram, there is a transition region where the convective envelope of a star turns into a radiative envelope. In the determination of the theoretical red edge of the δ Sct instability strip, there are some difficulties because of the interaction between convection and pulsation (Dupret et al. 2004). Therefore, it is important to derive accurate fundamental stellar and atmospheric parameters for δ Sct stars placed in this region. The δ Sct stars in eclipsing binaries are really essential for obtaining accurate fundamental parameters for further theoretical studies. Hence,

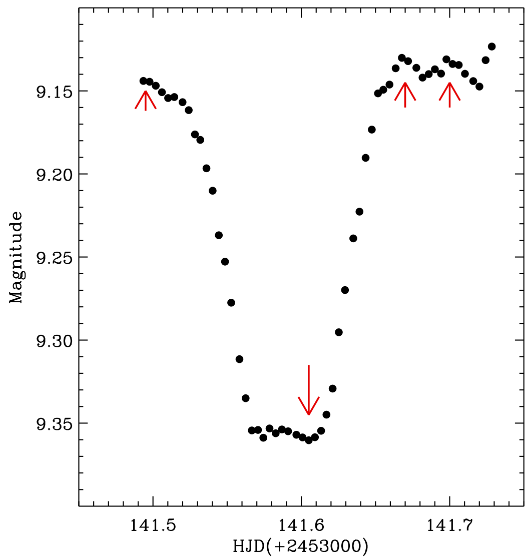

Fig. 9 Light variation of V948 Her.

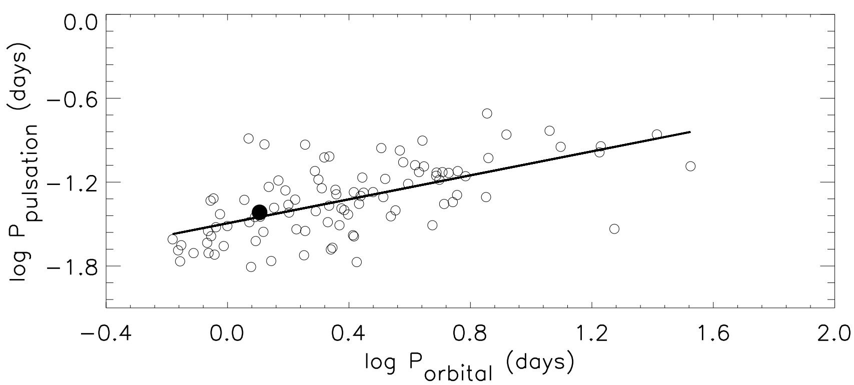

Fig. 10 The position of the primary pulsation component in the pulsation−orbital period relation (*solid line*). The filled circle represents the primary component. The other symbols show all δ Sct stars in eclipsing binaries and these data were taken from Kahraman Aliçavuş et al. (2017b).

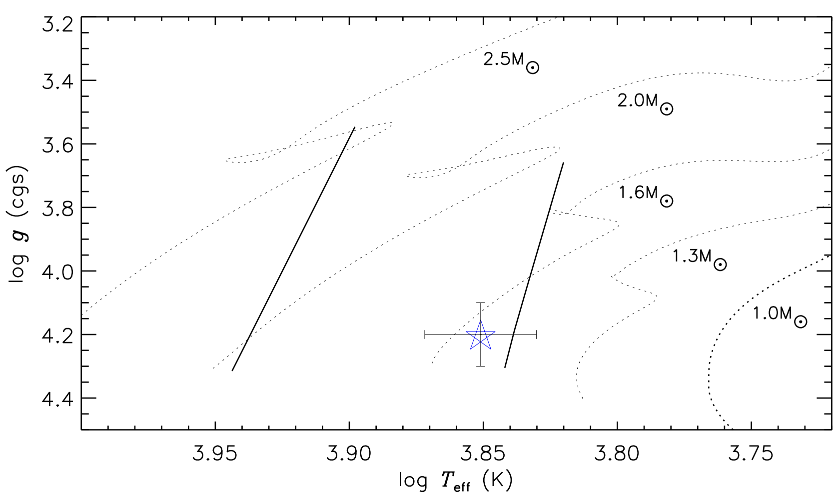

Fig. 11 The position of the primary component of V948 Her in the H-R diagram. *Dotted lines* are the evolution tracks for solar abundance and they were taken from Kahraman Aliçavuş et al. (2016). *Solid lines* represent the borders of the δ Sct instability strip (Dupret et al. 2005).

the present study of V948 Her will be an important contribution for further theoretical examinations.

Acknowledgements I would like to thank the reviewer for his/her useful comments and suggestions that helped to improve the publication. I thank Dr. F. Aliçavuş for his helpful comments. I am grateful to Dr. E. Niemczura, Dr. G. Catanzaro and Dr. D. Shulyak for putting their codes for the analysis of Fe lines, hydrogen lines and the calculation of $E(B - V)$ at my disposal. I thank Dr. J. Ostrowski for the evolution tracks. I thank the Çanakkale Onsekiz Mart University Research Foundation (Project No. FBA−2018−2452) for supporting this study. The calculations have been carried out in Wrocław Centre for Networking and Supercomputing (*http://www.wcss.pl)*, grant No. 214. This paper makes use of data from the first public release of the WASP data (Butters et al. 2010) as provided by the WASP consortium and services at the NASA Exoplanet Archive, which is operated by the California Institute of Technology, under contract with the National Aeronautics and Space Administration under the Exoplanet Exploration Program. This work has made use of data from the European Space Agency (ESA) mission Gaia (*http://www.cosmos.esa.int/gaia)*, processed by the Gaia Data Processing and Analysis Consortium (DPAC, *http://www.cosmos.esa.int/web/gaia/dpac/consortium*). Funding for the DPAC has been provided by national institutions, in particular the institutions participating in the Gaia Multilateral Agreement. This research has made use of the SIMBAD data base, operated at CDS, Strasbourg, France.

Appendix A:

Table A.1 Radial Velocities for the Primary Component of V948 Her

HJD 2450000 +	Orbital phase	v_{r} primary (km s^{-1})
2491.4213	0.1433	–70.535 ± 1.293
2302.6956	0.1468	–75.576 ± 1.700
1411.3368	0.1537	–72.109 ± 1.484
2491.5323	0.2303	–85.850 ± 1.088
1406.4243	0.3014	–83.951 ± 1.085
1739.3791	0.4006	–54.584 ± 0.767
1743.4511	0.5938	39.663 ± 0.601
1409.3839	0.6223	50.572 ± 1.203
1742.4267	0.7905	71.952 ± 1.122
1408.3965	0.8480	57.902 ± 0.987
1741.3929	0.9798	10.099 ± 1.327

References

Alfonso-Garzón, J., Montesinos, B., Moya, A., Mas-Hesse, J. M., & Martín-Ruiz, S. 2014, MNRAS, 443, 3022

Amôres, E. B., & Lépine, J. R. D. 2005, AJ, 130, 659

Asplund, M., Grevesse, N., Sauval, A. J., & Scott, P. 2009, ARA&A, 47, 481

Breger, M. 2000, in Astronomical Society of the Pacific Conference Series, 210, Delta Scuti and Related Stars, ed. M. Breger & M. Montgomery, 3

Butters, O. W., West, R. G., Anderson, D. R., et al. 2010, A&A, 520, L10

Chang, S.-W., Protopapas, P., Kim, D.-W., & Byun, Y.-I. 2013, AJ, 145, 132

Cox, A. N., Becker, S. A., & Pesnell, W. D. 2000, Theoretical Stellar Evolution, ed. A. N. Cox, Allen's Astrophysical Quantities, ed. A. N. Cox (New York: AIP Press; Springer), 499

Cutri, R. M., Skrutskie, M. F., van Dyk, S., et al. 2003, VizieR Online Data Catalog, 2246

da Silva, R., Maceroni, C., Gandolfi, D., Lehmann, H., & Hatzes, A. P. 2014, A&A, 565, A55

Duchêne, G., & Kraus, A. 2013, ARA&A, 51, 269

Dupret, M.-A., Grigahcène, A., Garrido, R., Gabriel, M., & Scuflaire, R. 2004, A&A, 414, L17

Dupret, M.-A., Grigahcène, A., Garrido, R., Gabriel, M., & Scuflaire, R. 2005, A&A, 435, 927

ESA. 1997, VizieR Online Data Catalog, 1239

Gaia Collaboration, Brown, A. G. A., Vallenari, A., et al. 2016, A&A, 595, A2

Gray, R. O., Corbally, C. J., Garrison, R. F., McFadden, M. T., & Robinson, P. E. 2003, AJ, 126, 2048

Iglesias-Marzoa, R., López-Morales, M., & Jesús Arévalo Morales, M. 2015, PASP, 127, 567

Ingber, L. 1996, Control and Cybernetics, 25, 33

Kahraman Aliçavuş, F., Niemczura, E., De Cat, P., et al. 2016, MNRAS, 458, 2307

Kahraman Aliçavuş, F., Niemczura, E., Polińska, M., et al. 2017a, MNRAS, 470, 4408

Kahraman Aliçavuş, F., Soydugan, E., Smalley, B., & Kubát, J. 2017b, MNRAS, 470, 915

Kjurkchieva, D., & Vasileva, D. 2018, New Astron., 58, 10

Koo, J.-R., Lee, J. W., & Hong, K. 2017, AJ, 154, 235

Kreiner, J. M. 2004, Acta Astronomica, 54, 207

Kurucz, R. L. 1993, SYNTHE Spectrum Synthesis Programs and Line Data (Cambridge, MA: Smithsonian Astrophysical Observatory)

Kurucz, R. L., & Avrett, E. H. 1981, SAO Special Report, 391

Liakos, A., & Niarchos, P. 2012, New Astron., 17, 634

Liakos, A., Niarchos, P., Soydugan, E., & Zasche, P. 2012, MNRAS, 422, 1250

Liakos, A., & Niarchos, P. 2017, MNRAS, 465, 1181

Liakos, A. 2017, A&A, 607, A85

Mermilliod, J.-C., Mermilliod, M., & Hauck, B. 1997, A&AS, 124, 349
Moultaka, J., Ilovaisky, S. A., Prugniel, P., & Soubiran, C. 2004, PASP, 116, 693
Pollacco, D. L., Skillen, I., Collier Cameron, A., et al. 2006, PASP, 118, 1407
Rodríguez, E., López-González, M. J., & López de Coca, P. 2000, A&AS, 144, 469
Ruciński, S. M. 1969, Acta Astronomica, 19, 245
Schlafly, E. F., & Finkbeiner, D. P. 2011, ApJ, 737, 103
Shokry, A., Saad, S. M., Hamdy, M. A., et al. 2018, New Astron., 59, 8
Soydugan, E., İbanoğlu, C., Soydugan, F., Akan, M. C., & Demircan, O. 2006a, MNRAS, 366, 1289
Soydugan, E., Soydugan, F., Demircan, O., & İbanoğlu, C. 2006b, MNRAS, 370, 2013
Udry, S., Mayor, M., & Queloz, D. 1999, in Astronomical Society of the Pacific Conference Series, 185, IAU Colloq. 170: Precise Stellar Radial Velocities, eds. J. B. Hearnshaw, & C. D. Scarfe, 367
van Hamme, W. 1993, AJ, 106, 2096
von Zeipel, H. 1924, MNRAS, 84, 665
Wilson, R. E., & Devinney, E. J. 1971, ApJ, 166, 605
Zhang, X. B., Luo, C. Q., & Fu, J. N. 2013, ApJ, 777, 77